npj | aging

Article

Published in partnership with the Japanese Society of Anti-Aging Medicine

https://doi.org/10.1038/s41514-026-00374-w

Individual differences reveal distinct age-related reorganizations in spatial channels for luminance and texture processing

Seung Hyun Min[1] ✉ & Alexandre Reynaud[2,3]

Aging impairs vision, but its specific impact on the neural channels underlying pattern processing is unknown. By examining individual differences in behavioral data from 52 younger and 50 older adults, we investigated how aging reorganizes underlying channels for detecting first-order (defined by luminance static or in motion) and second-order (defined by contrast, motion, or orientation) patterns. We identified a key organizational feature in youth on spatial processing: a global factor supporting all these pattern types at high spatial frequencies. Critically, this global factor was significantly weakened in older adults. Furthermore, high-frequency motion processing, which was integrated into this global factor in the young, became isolated and degraded with age. In contrast, orientation processing was spared, possibly reflecting distinct age-related changes in its spatial channels. Lastly, a two-channel system was found to govern all second-order patterns in both age groups. Our findings reveal a neural signature of sensory aging: a deterioration in global integration for pattern processing and a specific vulnerability in motion-defined pattern processing, while orientation-defined pattern processing is maintained through distinct organizational changes. The present findings extend neural dedifferentiation frameworks in cognitive aging to the organization of spatial frequency channels in pattern vision.

The human visual system has a remarkable ability in detecting various types of patterns. For example, we can easily distinguish a city skyline against the sky because buildings create clear luminance variations—a process known as first-order (luminance-modulated (LM)) processing in early visual areas. However, telling apart individual buildings requires analyzing finer texture differences, such as window arrangements or movements behind glass—a task involving second-order processing in early and late visual cortex. These sensory processes, however, decline with age even without ocular pathology, creating growing challenges as the global population over 60 is projected to double by 2050[1]. Understanding these age-related changes requires examining how neural processing of both luminance and texture information becomes altered.

Contrast sensitivity studies have established that aging primarily targets high spatial frequencies, with seminal works attributing this decline to combined optical and neural factors after age 40–50[2–4]. Previous research suggests that sensitivity for luminance and texture patterns deteriorate independently[5], with unique progression rates[6] across different stimulus types. These dissociations likely reflect distinct cortical pathways governing first- and second-order sensitivity in striate[7,8] and extrastriate visual areas[9–11], supported by the standard cortical two-stage filter-rectify-filter model for second-order processing[8,10,12]. This model engages both early and higher visual areas, forming intricate foundations for complex vision, including perceiving natural scenes and faces. While studies have reported that aging differentially influences sensitivity for different patterns (first- and second-order images), there is no framework describing how these spatial processes are globally organized and mediate such age-related changes in both global and local organization of these processing pathways.

The distinction among general decrease in sensitivity across stimulus types, pathway-specific alterations of spatial channels, or their global organization between these unique processes is crucial for understanding

[1]Department of Psychology, Zhejiang Sci-Tech University, Hangzhou, China. [2]McGill Vision Research, Department of Ophthalmology and Visual Sciences, McGill University, Montreal, Canada. [3]Centre for Digital Brain Therapies, BRaIN Program, Research Institute of the McGill University Health Centre, Montreal, Canada. ✉e-mail: seung.min@zstu.edu.cn

how aging impacts basic building blocks of spatial vision. However, the neural substrates of these aging patterns remain poorly understood. Prior works have examined patterns of individual differences across a wide range of spatial parameters to derive channel properties in contrast perception, color, and stereopsis[13–19] in both healthy[20] and clinical populations[21]. Additionally, other studies have used adaptation and masking paradigms to reveal first-order[22] and second-order channels in human observers[23,24]. However, multiple stimulus types have not been studied systematically with identical spatial parameters to identify spatial channels for first- and second-order processing because of methodological limitations in measuring visual functions across different pathways. Identifying latent sources of individual differences in data requires multivariate statistical methods that work reliably with large datasets with paired observations across stimulus types and spatial frequencies. This is now possible due to modern software packages for data analysis and modeling, as well as recent developments in psychophysical testing, such as the quick Contrast Sensitivity Function (*qCSF*) method[5,25–27].

Here, we seek to understand the global organization of spatial channels —defined as their shared structure across stimulus types—that process first- and second-order stimulus types across wide ranges of spatial frequencies, the local organization of these channels within each stimulus type, and examine their both the global and local age-related changes using population datasets of individuals with normal vision. We address these questions through a novel combination of factor analysis and computational modeling applied to comprehensive datasets of contrast sensitivity for both first-order (oriented and moving LM, 1–14.16 c/deg) and second-order stimuli (contrast-, motion-, and orientation-modulated, 0.25–3.54 c/deg) in 52 young and 50 old visually intact observers. We hypothesize that aging not only reduces sensitivity for first- and second-order processing but also alters how these distinct processes interact with each other, as well as modify the properties of spatial channels that subserve each process.

Results

Sensitivities to some patterns are more susceptible to aging than others

In their previous study, Reynaud et al. examined sensitivity from 52 young observers and 50 older subjects, all of whom had normal visual acuity for first- and second-order visual stimuli (each shown in Fig. 1A). They observed that peak sensitivity, which is the maximum sensitivity across tested spatial frequency ranges, for oriented and moving first-order LM patterns similarly declined with age. For second-order stimulus types, peak sensitivity for orientation-modulated (OM) signals remained spared despite aging, while two other second-order stimuli—contrast-modulated (CM) and motion-modulated (MM)–showed similarly significant reductions, with MM exhibiting the lowest peak sensitivity relative to CM and OM. Together, peak OM sensitivity remained intact (green curve in Fig. 1A), while other peaks declined significantly with aging.

Importantly, although CSFs characterize the overall shape of sensitivity across spatial frequencies, they do not capture how sensitivities co-vary across individuals and therefore cannot reveal the underlying covariance structure. Beyond examining mean sensitivity, multivariate analysis of individual differences in behavioral data could reveal how different processes could interact and elucidate if aging could alter these relationships between separate processes, often reflected in clustered correlation matrices[16,19,28]. We observed similarly clustered correlation patterns in young and older groups (Fig. 1B). Sensitivity for each stimulus type was strongly correlated at nearby frequencies (evident along the matrix diagonals), and some stimulus types showed selective relationships. Both groups exhibited strong correlations at all spatial frequencies between the two first-order stimuli (oriented and moving LM), but more robust in older subjects (Fig. 1B, right). Interestingly, the correlation patterns among second-order stimuli types (e.g., MM and CM/OM) are slightly different. Correlations are mostly present at low frequencies and stronger in young observers (Fig. 1B, left) than in older individuals (Fig. 1B, right). These group differences that could possibly reflect age-related reorganization are examined in detail using factor analysis in subsequent sections.

Aging weakens the global relationship between spatial channels for processing luminance and texture patterns

To explore age-related changes of the prominent correlation patterns in Fig. 1B and identify latent sources of individual differences in sensitivity across stimulus types and spatial frequencies in each subject group, we decomposed the prominent correlation patterns into distinct components using factor analysis on the combined dataset for each age group. Strong correlation patterns suggest the influence of shared underlying factors, while the absence of correlations implies distinct mechanisms. This approach allowed us to determine how many factors govern sensitivity for first- and second-order signals and understand how these factors change with age, providing insights into the neural mechanisms underlying pattern perception.

For each group, factor analysis extracted seven significant factors based on the Guttman criterion (eigenvalues > 1; scree plots in Fig. 1C). Although alternative methods suggested five (parallel analysis) or nine factors (systematic factor loadings), we selected seven as an intermediate solution from the Guttman criterion (see Table S1). This decision was further supported by the nine-factor model, producing a weakly loaded, potentially extraneous factor in older subjects (Fig. S1). Additionally, the seven-factor model confirmed two distinct first-order factors above 1 c/deg in both age groups, consistent with our prior work on a different dataset[20]. The model accounted for 85.0% of cumulative variance in young and older individuals and exhibited minimal residuals (Fig. S2). Figures 2, 3 display factor loadings and correlation structures for each factor in young and older adults (factor loading values in Tables S2 and S3), ordered by variance explained and loading scores, and color-coded by stimulus type. Factor loadings are displayed in polar plots (radius: loading values; circumference: spatial frequency in clockwise direction; see bottom-right guide panel in Fig. 2) to visually demonstrate how channels for different stimulus types can operate together (i.e., polar plots where loadings are significant for several stimulus types, such as Factor 1 in Fig. 2) while some others operate independently within specific frequency ranges (i.e., polar plot where loadings are significant for mainly one stimulus type, such as Factor 4 in Fig. 2). The correlation structure for each factor (displayed as a heatmap) shows how the complex pattern of correlations in our original, empirical data (Fig. 1A) can be broken down into simpler, meaningful components. The purpose of these correlation plots is to demonstrate that the factor model is comprehensive; when the correlation patterns from all seven factors are combined, they faithfully reconstruct the prominent correlations seen in the raw data without overlooking significant relationships (Fig. S2). This validation, as used in previous studies[15,18], confirms that the seven-factor solution successfully captures the core patterns of individual differences in each age group.

In young adults, the seven-factor model revealed one factor that accounted for global relationships across spatial channels for first- and second-order stimulus types, and six factors that operated independently within a specific frequency range of one stimulus type. Factor 1 (26.5% variance) was associated with sensitivity for all first- and second-order stimuli at high frequencies; although the loadings are barely larger than 0.5 for the OM stimuli. This aligns with evidence that first- and second-order processing, though distinct, interact at early stages[7,29].

In contrast to high-frequency channels, low-frequency channels are all loaded on different factors. For first-order luminance modulated stimuli, the moving LM low-frequency channel is loaded on Factor 2 (14.0%), and oriented LM low-frequency is loaded on Factor 7 (6.6%). Second-order processing, low-frequency processing channels are also governed by distinct factors. MM low-frequency processing is loaded on Factor 3 (10.3%), CM low-frequency is loaded on Factor 5 (10.1%). Unlike other stimuli, OM was less dependent on Factor 1, with low-frequency sensitivity loaded on Factor 4 (10.2%) and high-frequency loaded on Factor 6 (7.4%).

These results highlight key findings about the organization of these spatial channels in young populations. Two separate spatial

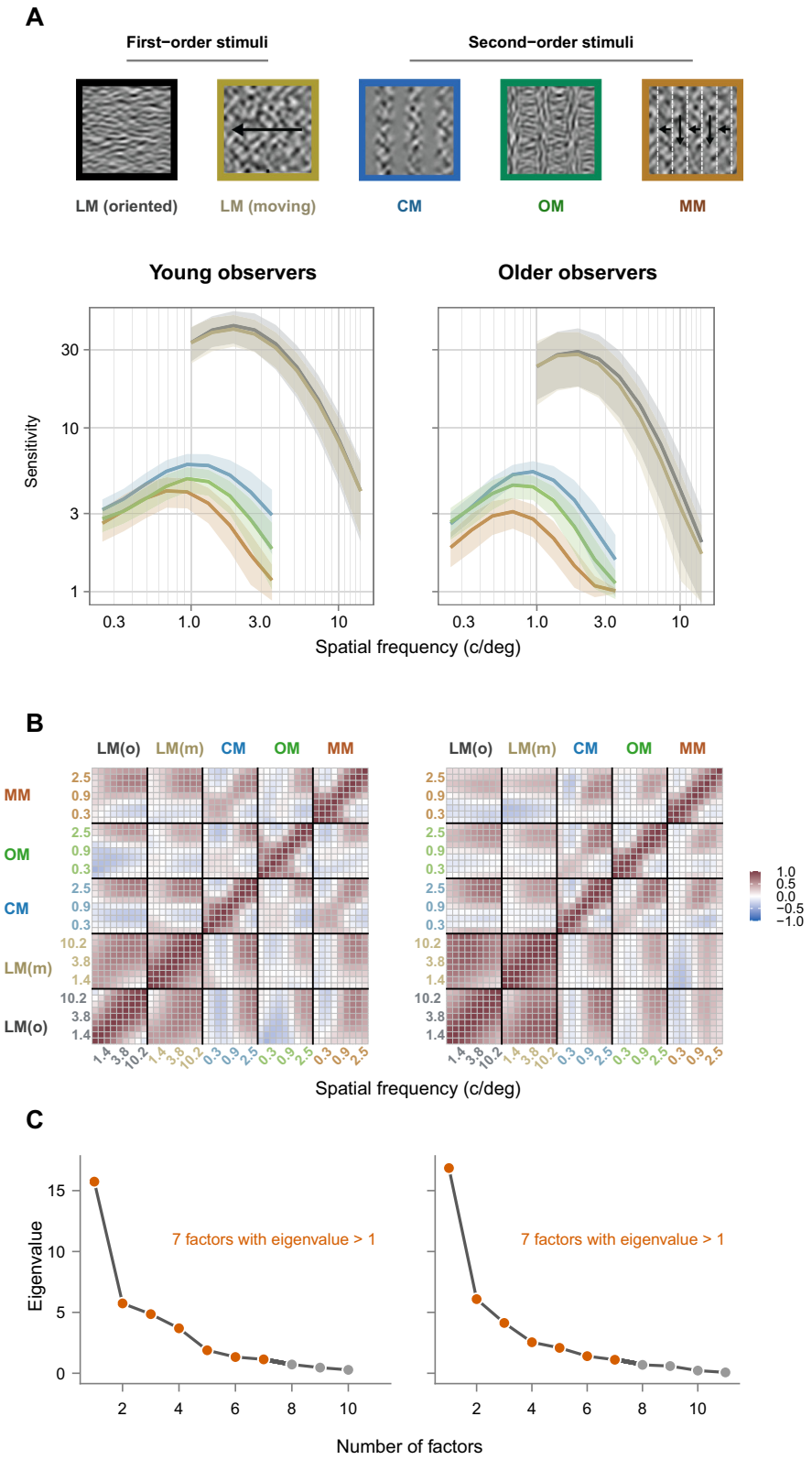

Fig. 1 | Individual differences in sensitivity for first- and second-order patterns reflect hidden, latent sources of variability. Data of young observers are shown in the left column, while data of old participants are displayed in the right column. **A** Five stimulus types used in this study. Oriented and moving first-order luminance-modulated (LM) sensitivity was measured in at 1–14.16 c/deg, while second-order contrast-, orientation-, and motion-modulated (CM/OM/MM) sensitivity was measured at 0.25–3.54 c/deg using the validated *qCSF* method. Mean sensitivity data with standard deviations in shades shown for each stimulus type and subject group (52 young observers, 50 older observers). **B** Correlation matrix from empirical data for each subject group reveals systematic patterns, with significant correlations observed along the diagonal of the matrix. There are also significant correlation patterns far from the diagonal, reflecting common mechanisms among different stimulus types. **C** Scree plots indicating that solutions with seven factors (orange points, eigenvalues > 1) are adequate to describe correlation patterns in data of young and older groups. Of 45 available variables in the datasets, only factors with eigenvalues above 0 are plotted for each group's scree plot, with gray points representing insignificant factors with eigenvalues between 0 and 1.

channels exist for each stimulus type. While visual processing involves separate pathways for low-frequency processing, as reflected by a unique low-frequency channel for each stimulus, high-frequency processing shares a common spatial channel across all stimulus types except OM signals. This indicates that OM processing is segregated at all frequencies, while second-order CM and MM processing correlate with first-order sensitivity at high frequencies but diverge at low frequencies.

In older individuals, the factor model reveals a reorganized structure of visual processing that shares some features with younger observers but also shows key differences. Similar to younger adults, high-spatial frequency sensitivities for all stimulus types are represented by a single factor (Factor 2:

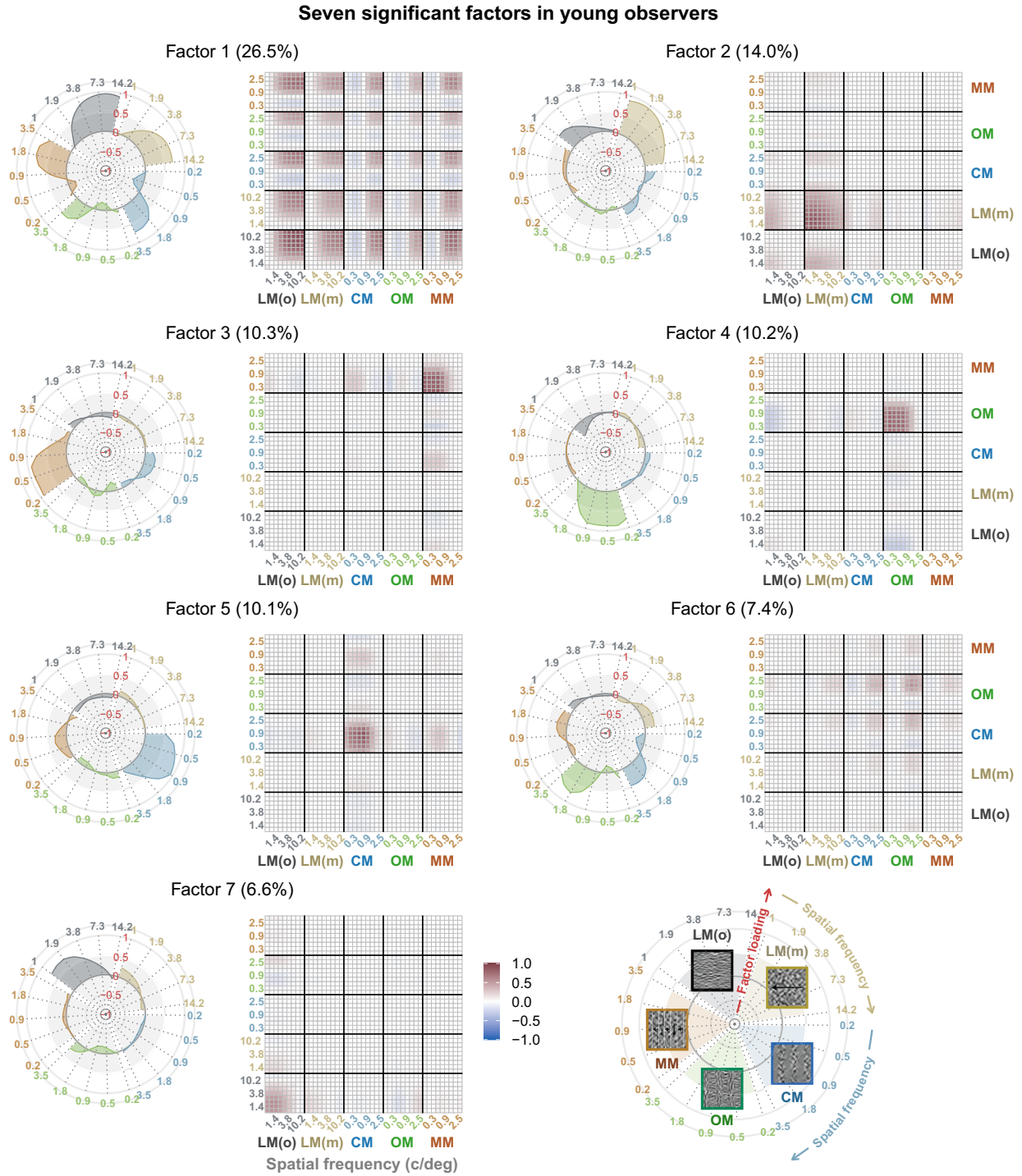

Fig. 2 | Factor analysis on sensitivity data across five stimulus types in young observers reveals that seven factors can capture individual differences in raw data. The polar plots on the left show each factor loading (radius) across spatial frequency (circumference in clockwise direction, as indicated in the bottom-right guide panel). The thick light-gray line shows a reference loading score of 0. The proportion of variance for each factor is also reported on each plot. Correlation heatmap shows the correlation coefficient among all tested conditions, where dark red color denotes strong, positive correlations. The plots for loadings have been color-coded based on stimulus types. LM luminance-modulated, CM contrast-modulated, OM orientation-modulated, MM motion-modulated.

15.8%), and second-order processing remained loaded on individual, dedicated factors for each type. However, the organization of low-frequency pathways was altered. Unlike in younger subjects, both low-frequency LM stimuli (static and moving) were consolidated into a single factor (Factor 1, 23.9%), indicating a reorganization that brings these static and motion pathways closer together. A further key change was observed in the high-frequency processing of second-order stimuli: while OM sensitivity maintained its own dedicated high-frequency factor (Factor 7: 8.1%) as in younger adults, MM processing at high frequencies also became governed by a separate, dedicated factor (Factor 3, 10.4%) rather than being integrated into the global high-frequency factor. Here, integration refers to the extent to which sensitivities across different stimulus types load onto a common latent factor, reflecting shared variance across processing channels.

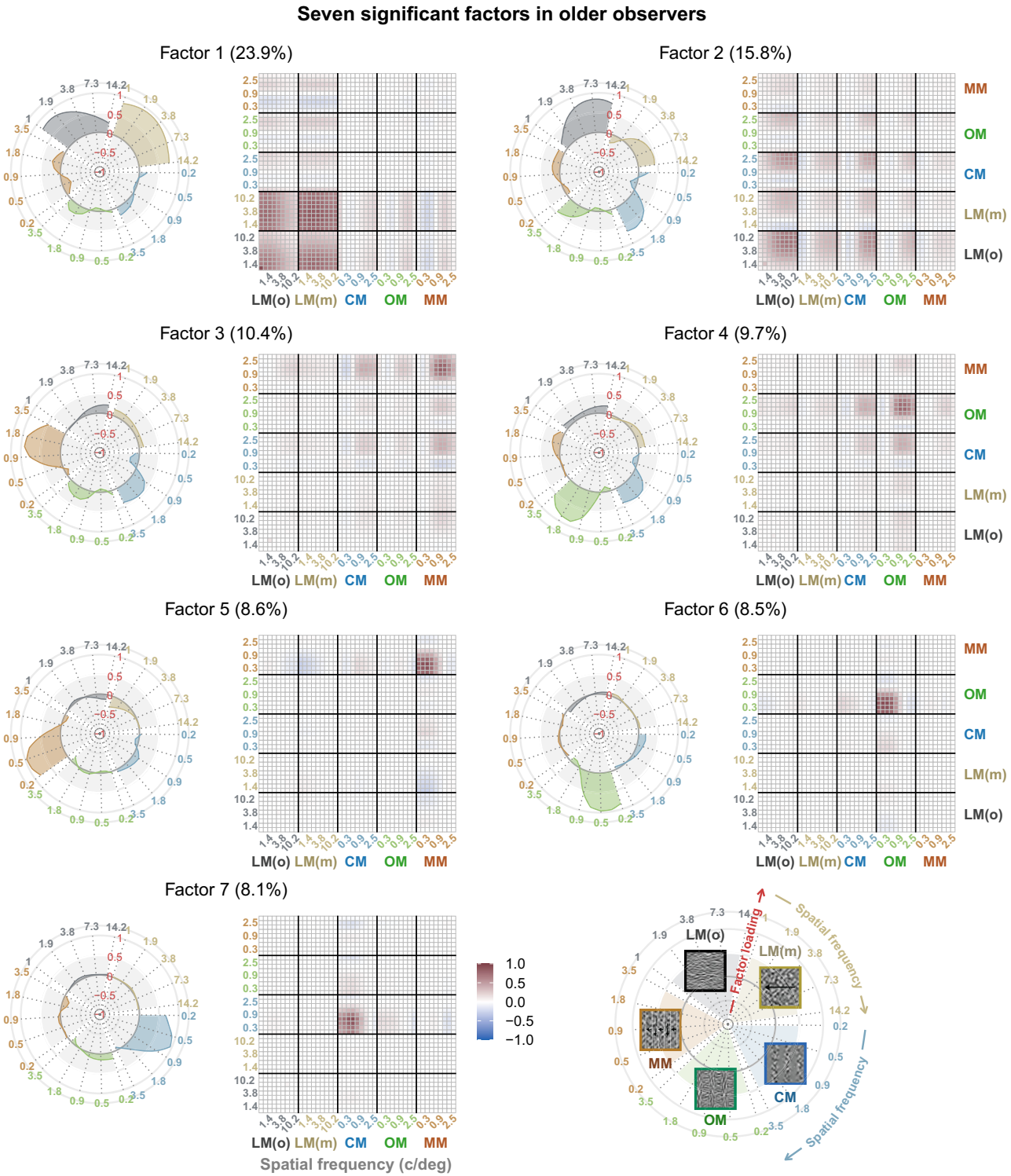

Fig. 3 | Factor analysis on sensitivity data across five stimulus types in older observers showed that seven factors can adequately account for the variance of the data. Loadings for each factor and correlation structure of the original data explained by each factor are displayed similarly to Fig. 2. LM luminance-modulated, CM contrast-modulated, OM orientation-modulated, MM motion-modulated.

This suggests a reduction in integration and a shift toward more localized, stimulus-specific processing with age.

Our finding that high-frequency MM processing becomes more isolated in older adults could, in principle, be explained by increased measurement variability from reduced sensitivity, leading to lower correlations with other stimulus types. To evaluate this possibility, we estimated measurement reliability using inter-eye Spearman–Brown correlations (treating the two eyes as parallel test halves), examined floor effects, and conducted sensitivity analyses. At the frequencies where MM loaded most strongly on Factor 3—and was therefore most isolated from the global factor (1.31–1.83 cpd; Table S3)—MM in older adults demonstrated reliability (Spearman–Brown = 0.765–0.775; Table S6) comparable to CM (0.769–0.794) and OM (0.605–0.698). Floor effects for MM were modest (1–18% at 1.31–1.83 cpd; Table S7), although slightly higher than for CM

(0%) and OM (0%). Sensitivity analysis by removing MM thresholds at 2.54 and 3.54 c/deg, where floor rates were elevated (>60%; Table S7), and recomputing the same factor structure in older adults revealed that MM at 0.94, 1.31 and 1.83 c/deg continued to load on a factor (Factor 4 in Table S8) distinct from the global high-frequency factor (Factor 2 in Table S8), as in our original factor structure (Fig. 3 and Table S3). These results collectively indicate that the observed MM isolation is unlikely to be driven solely by measurement artifact and instead reflects age-related reorganization of spatial channels.

Both age groups showed one factor representing broad sensitivity covariance across stimulus types at high frequencies—Factor 1 in young observers (Fig. 2) and Factor 2 in older subjects (Fig. 3). Alongside the global factor, other factors were associated with one stimulus type and a specific range of spatial frequency. To examine the strength of the correlation patterns in the global factor in both age groups, we visualized six-factor solutions without the global factor in correlation matrices, revealing that this factor was essential for preserving the patterns in the data of young observers but unnecessary for older subjects (Fig. S3). This indicates that while young observers show strong interactions between first- and second-order processing at high frequencies, these relationships weaken with age, resulting in more isolated processing channels. This age-related reorganization may also partially explain the specific loss of high-frequency second-order sensitivity observed in older individuals[5,30] stemming from weakened global relationship with first-order processing.

Finally, to determine if the latent factor structure of sensitivity differed significantly between age groups, we conducted a multi-group confirmatory factor analysis. We tested a sequence of nested models to assess measurement invariance: a configural model (equal factor structure; i.e., seven-factor solution from young observers), a metric invariance model (equal factor loadings), and a scalar invariance model (equal loadings and intercepts). Likelihood Ratio Tests (Table S4) revealed that constraining factor loadings to be equal significantly worsened model fit ($\Delta\chi^2(40) = 74.30$, $p < 0.001$), indicating that the strength of the relationships between latent factors and their sensitivity measures differed by age. Furthermore, constraining both loadings and intercepts resulted in a more substantial degradation of fit ($\Delta\chi^2(37) = 357.06$, $p < 0.001$), demonstrating that the groups also differed in their baseline performance. These results indicate that factor structures are fundamentally different between young and old groups, reflecting age-related differences in the functional organization of spatial channels. Consequently, separate factor analyses for each age group (Figs. 2, 3) are not only justified but also statistically necessary.

Age-related alterations in low- and high-frequency channels are unique across stimulus types

Combined factor analysis with the seven-factor model suggested there is one low-frequency and one high-frequency spatial channel for sensitivity in each stimulus type in both age groups. To validate this observation, we applied standard factor extraction methods (parallel analysis, Guttman criterion, and systematic loadings) for each separate type in each group, which predominantly identified two significant factors (Table S5).

We then performed separate factor analyses using two-factor models for each stimulus type and age group to extract specific channel loading patterns. Factor loadings are displayed in Fig. 4A, indicating that the tested range of spatial frequency is subserved by two separate channels for all five stimulus types. These loading scores were slightly different from those provided in polar plots from Figs. 2, 3 (values in Tables S2 and S3), which are derived from combined factor analysis for each group. For first-order stimuli (oriented and moving LM), older observers showed channels operating across broader frequency ranges compared to younger subjects (minimum loading scores near 0 in young but 0.25 in aged), showing age-related de-differentiation of LM spatial channels. Aging effects in second-order processing were particularly notable: older subjects exhibited narrower ranges of robust loading scores in low-frequency channels, but broader ranges of robust loading scores in high-frequency channels, especially for OM processing, whose peak sensitivity remained spared (see Fig. 1A). This high-frequency expansion of first- and second-order spatial channels may represent adaptive reorganization associated with maintained sensitivity.

While loading scores in Fig. 4A provided a qualitative visualization of channel interactions, we quantitatively characterized these channels by fitting Wilson's spatial model to each subject's data. The resulting tuning curves for different stimulus types are plotted in Fig. 4B, showing how two factors for each stimulus type can subserve a specific range of spatial frequency. We also observed that there was a specific frequency value where the two channels would intersect (arrows in Fig. 4B). This intersection point was derived for each subject, and the average was computed (see Fig. 4C for mean and individual scatter points). Bonferroni-corrected pairwise t-test revealed significant differences in intersections across all stimulus types (p's ≤ 0.0007) between age groups. Among second-order stimuli, OM intersection showed the most pronounced shift towards lower frequencies (Cohen's $d = 8.03$; Fig. 4C), agreeing with the loading patterns in Fig. 4A. Notably, while moving LM channels appeared stable in the loading score patterns despite aging (Fig. 4A), their tuning curves showed significant changes in their position of intersections (Fig. 4C), demonstrating that aging systematically alters the properties and overlapping areas of spatial channels for pattern detection. Intersections between oriented LM channels significantly increased after aging, while those between other stimulus channels significantly reduced (Fig. 4C), indicating that different types of LM stimulus could have unique aging effects at the level of spatial channels in the visual system.

Discussion

This study investigated how aging affects sensitivity across spatial frequencies and visual pathways by examining LM (first-order) and texture-defined (second-order) pattern processing in younger and older adults. We used factor analysis, a multivariate analysis method that can uncover latent sources of variability in individual differences, to reanalyze previously obtained sensitivity data in young[27] and older populations[5]. We observed that sensitivity is governed by two low- and high-spatial frequency channels for all second-order stimulus types (CM, OM, MM) in both younger and older adults. However, we found distinct organizational differences between age groups. The correlation structures in behavioral responses revealed that different second-order image types are processed separately in both age groups, consistent with their established independent neural mechanisms[31,32]. Younger adults showed robust neural integration of pattern processing, with a single dominant factor explaining sensitivity variance across all stimulus types (first- and second-order) at high frequencies. In older observers, we also identified a single global factor underlying LM, CM, and OM patterns at high frequencies. However, this factor accounted for a much smaller proportion of the raw data's variance (15.8%) compared to young observers (26.5%). Furthermore, MM processing was found to be isolated from the global factor, reflecting a more fragmented process for perceiving motion patterns. This suggests that aging affects not only sensitivity for first- and second-order stimulus but also impacts how these processes co-exist in the visual system, leading to sensitivity variability in older adults that reflects a more localized processing.

From our data, a fundamental neural organization of spatial channel was observed: for all second-order stimulus types (CM, OM, and MM), sensitivity is governed by two spatial channels, low- and high-frequency, in both younger and older adults. This finding aligns with the established two-channel model found in other visual modalities. Chromatic sensitivity (red-green and blue–yellow)[13,14,20,33] is subserved by two spatial channels, reflecting the low-pass properties of chromatic CSF. Similarly, stereopsis relies on two primary disparity channels tuned to low and high spatial frequencies[17,19]. All these studies reveal that channels have a bandwidth of about 2 octaves each. In contrast, achromatic (luminance) processing requires a third, higher-frequency channel to capture its wider full spatial range[20], a difference potentially driven by optical factors[34]. The consistent emergence of a two-channel system across these diverse visual

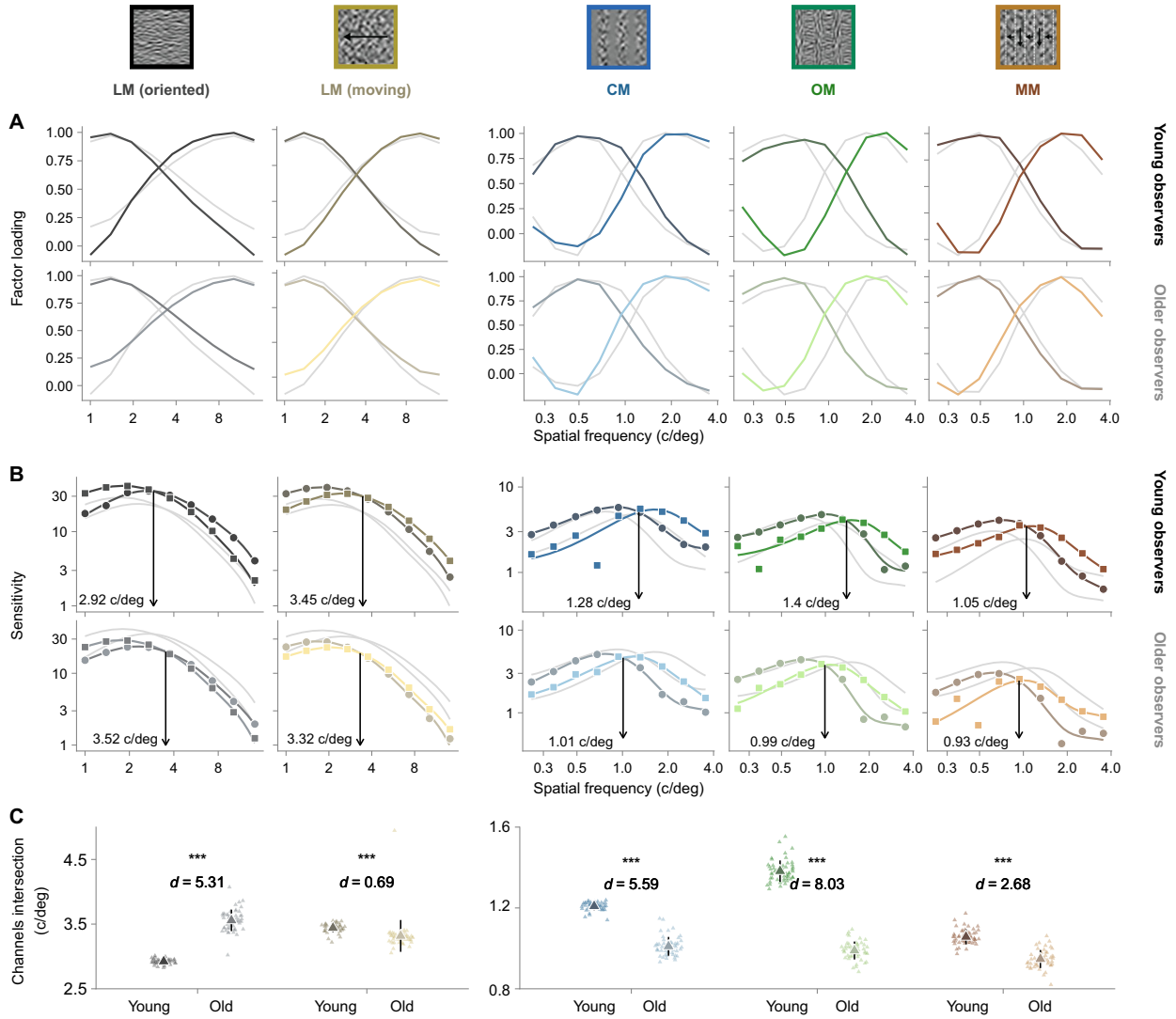

Fig. 4 | Results from separate factor analysis for each stimulus type (represented in each column) and age group (young and old populations). The ghost gray traces in each panel represent the data of the other age group to allow direct comparisons for readers. Saturated color schemes represent data of young observers, while slightly de-saturated color palettes denote the sensitivity of older subjects. **A** Loading scores of two spatial channels for each stimulus type and age group. **B** Tuning functions for low- and high-frequency spatial channels across five stimulus types in young and older individuals. **C** A plot displaying average and individual locations of where low- and high-frequency channels intersect. Asterisks indicate statistical significance from pairwise comparisons with Bonferroni corrections (***$p < 0.001$). LM luminance-modulated, CM contrast-modulated, OM orientation-modulated, MM motion-modulated.

modalities—texture, color, and depth—could suggest a common neural organization in the visual system for processing non-luminance-based information. This may stem from their shared lowpass characteristics, for which a dual-channel system is sufficient.

However, separate factor analyses revealed stimulus-specific age effects on channel organization. To begin with, first-order channels between two LM types showed unique age-related changes even if their only difference was the presence (moving LM) or absence of motion (oriented LM). Oriented LM channels showed increased intersection positions between frequency ranges, while moving LM channels demonstrated decreased intersections—a pattern surprisingly similar to second-order MM channels (Fig. 4B). This parallel progression in motion-processing channels occurs despite their known unique neural mechanisms[35], suggesting shared age-related modifications across motion processing pathways for detecting first- and second-order patterns.

Additionally, our analysis revealed distinct age-related changes in low- and high-frequency channels for second-order processing. While CM, OM, and MM stimuli all showed similar directional shifts—with high-frequency channels broadening their frequency ranges and low-frequency channels narrowing their ranges—OM channels exhibited the most pronounced changes in both correlation structures and tuning functions. This substantial reorganization of OM channels coincides with preserved peak sensitivity for OM perception in older adults, contrasting with the significant reductions observed for CM and MM sensitivity (Fig. 1A). Whether this reorganization reflects compensatory mechanisms or other age-related processes remains to be determined. The relative preservation of OM processing, which can involve ventral extrastriate pathways including V2[36], LO1, hV4, VO1[9,11,37], and V4[38], aligns with previous reports of maintained orientation detection thresholds in aging[39–41]. The spared OM processing may stem from not only OM's significant shifts in their channel intersections, but also its inherent independence from first-order high-frequency sensitivity in young observers (lower loading scores for OM in Factor 1 and independent OM Factors 4 and 6 in

Fig. 2), potentially insulating it from age-related declines in LM processing that more strongly affect CM and MM sensitivity due to their clustered correlations.

Conversely, MM processing showed increasing isolation in older observers, particularly at high spatial frequencies. This was evidenced by the global factor (i.e., Factor 2 in Fig. 3) incorporating high-frequency LM, CM and OM processing but excluding MM, which instead relied on separate dedicated factors (Factors 3 and 5 in Fig. 3). This segregated organization differs markedly from young observers, where a single global factor (i.e., Factor 1 in Fig. 2) was associated with all stimulus types at high frequencies. The localization of MM processing may relate to its particularly vulnerable sensitivity profile, showing both the lowest peak frequency among all stimuli (Fig. 1A). A previous study reports that this global factor, which is associated with high frequency LM sensitivity (above 2.25 c/deg), is related to the state of optics because it can be entirely removed with adaptive optical correction[34]. Together, there is a possibility that the age-related changes in the global source of variability, notably its weakening relationship with high-frequency MM signaling, are driven by optical shifts. Nevertheless, the aging visual system seems to have undergone neural changes to create separate sources of variability for high-frequency MM signaling rather than just losing its functionality. This neural reorganization—the creation of separate sources of variability for high-frequency MM processing—may be associated with preservation of motion-defined pattern perception in the face of age-related optical and neural changes. This process could involve functional changes in V1[12] and extrastriate areas like V3[42] and other higher temporal regions[43]. This dual susceptibility—combining sensitivity loss with neural isolation—makes MM processing uniquely vulnerable to aging among second-order stimuli, potentially highlighting the need for motion-stream specific therapy to prevent age-related visual decline.

The present findings also bear a relationship to neural dedifferentiation in cognitive aging[44–46], which refers to reduced functional specificity and broader tuning of neural representations in older adults[47]. Older observers exhibited broader loading ranges for first-order LM stimuli across spatial frequency (Fig. 4A) compared to young populations, indicating that spatial frequency specificity is markedly reduced. In addition, the global high-frequency factor identified in older observers (Factor 2 in Fig. 3) was substantially less dominant (15.8% proportion of variance) than in younger observers (26.5%; Factor 1 in Fig. 2). This reduced cross-stimulus covariance at high spatial frequencies indicates weakened integration between first- and second-order processing channels with age. Importantly, high-frequency MM processing became increasingly isolated compared to other second-order stimulus types, reflecting stimulus-selective reorganization with aging[48]. Although these results are based on behavioral covariance rather than neural measures, the reduced shared structure across stimulus types and stimulus-specific isolation parallel reports of diminished functional integration and altered segregation in aging visual and large-scale brain networks[49–52].

Previous studies have applied factor analyses across heterogeneous visual tasks to examine whether visual abilities share a common general factor[53–55]. For example, Shaqiri et al.[55] reported weak inter-task correlations in both young and older adults, concluding that visual abilities decline relatively independently. The present study focuses on pattern sensitivity and explicitly models the latent organization of spatial frequency channels within first- and second-order systems to examine how the internal channel structure of pattern vision is reorganized with age, both within individual stimulus types and across pattern types.

The physiological basis for the observed weakening of global integration and stimulus-specific shifts in spatial channel tuning may involve age-related alterations in neurochemistry within the visual cortex. Animal studies show reduced GABAergic signaling in aging visual systems[56,57], impairing critical functions like orientation selectivity[58] and center-surround suppression[59,60]—the latter of which is essential for second-order processing in V1 and V2[61]. Reduced inhibition could thus plausibly contribute to the channel reorganization observed here. However, direct evidence from human neuroimaging is mixed. Using magnetic resonance spectroscopy, Pitchaimuthu et al.[62] found increased GABA+ levels in the visual cortex of older adults, contrary to previous animal studies, and further observed that higher GABA+ correlated with reduced perceptual surround suppression. This challenges a simple one-to-one mapping between inhibitory neurochemistry and inhibition-related perceptual performance[63]. Alternatively, glutamate/glutamine (Glx) and GABA concentrations are relatively balanced and correlated in the human cortex[64], and perceptual changes can scale with the magnitude of neurochemical deviations[65]. Age-related perceptual changes may therefore reflect disruptions in this equilibrium—particularly if GABA exhibits larger age-related shifts than Glx in visual cortex[62]—rather than a simple one-to-one mapping between GABA concentration and inhibitory function.

Shared covariance in contrast sensitivity measures does not uniquely index sensory channel organization. Here, factor analysis captures behavioral covariance patterns rather than physiological mechanisms, and contrast sensitivity reflects multiple influences beyond spatial tuning, including internal noise[66], perceptual efficiency[67], decision processes[68], and attentional modulation[69], all of which are affected by aging[70–72]. Thus, although our analyses show that the covariance structure of luminance and texture processing differs with age, they cannot determine whether these changes arise from sensory reorganization or age-related alterations in noise, attention, or decision processes that affect covariance in sensitivity. Due to stimulus design, first- and second-order stimuli were necessarily tested over partially different spatial frequency ranges (1–14.16 c/deg in first-order vs. 0.25–3.54 c/deg in second-order), specifically due to the fixed 1:4 spatial frequency ratio between the carrier and envelope[5,27]. Although this difference may have influenced the factor-analytic results, we believe that this design choice was necessary because second-order processing is more lowpass[30,73]. Including spatial frequency ranges at which sensitivity approaches zero would introduce statistical artifacts, such as floor effect and unstable or weak factor loadings, in factor analysis[74,75].

In our studies, motion stimuli were presented at a temporal frequency of 2 Hz, which is close to the peak of human temporal sensitivity[76] and to the preferred temporal tuning of neurons in primary visual cortex[77], which provide input to second-order processing mechanisms in the classical filter-rectify-filter model[8,12]. Since age-related declines are often more pronounced at higher temporal frequencies or velocities[3,78,79], selecting a near-optimal temporal frequency reduces the likelihood that observed thresholds for texture patterns are driven primarily by first-order temporal limitations. Notably, at higher temporal frequencies, age-related declines in first-order temporal sensitivity may propagate to second-order thresholds, making the two sources of decline difficult to disentangle. A substantially larger and more comprehensive dataset would be required to characterize age effects across the full spatiotemporal domain[80] and to directly map these interactions.

Sex distribution was closely balanced across age groups (young: 25/52 females; older: 28/50 females). While robust sex differences in contrast sensitivity thresholds are generally not observed[81,82], sex differences have been reported in motion perception in favor of males[82–84], and motion functions decline with age[3,85]. However, sex was not modeled in the factor analyses, and potential sex-by-age interactions cannot be ruled out. Consequently, it is possible that unmodeled sex-related variability could influence the factor structure underlying sensitivity to motion-based stimuli (moving LM and MM).

In conclusion, our results reveal that aging induces significant reorganizations of spatial channels across both first- and second-order processing, manifesting through both local and global modifications. At the systematic level, we observed a pronounced weakening in the relationship between high-frequency channels for first- and second-order processing. For first-order pathways, changes include increased correlations between low- and high-frequency channels for moving LM signals, and merged processing of static and moving LM images at low frequencies in older populations. Second-order processing shows stimulus-specific alterations: MM becomes mechanistically isolated, particularly at high frequencies, from both first- and other second-order stimulus types, while OM channels

undergo substantial positional shifts that accompany maintained sensitivity. These differential patterns of reorganization highlight the visual system's varied adaptive responses to aging, where some pathways demonstrate functional decline while others exhibit potential preservation strategies.

Methods

Participants and procedure

In this study, we analyzed two datasets from previously published studies[5,27] with a total of 102 observers who completed testing at multiple spatial frequencies for multiple types of stimuli. The two datasets included contrast sensitivity data for first-order (oriented and moving LM patterns) and second-order (CM, MM, and OM) for the dominant and non-dominant eyes from 52 normally sighted young observers (27 males and 25 females; average age = 24.9 ± 0.3 years; age range = 21–30 years)[27] and 50 aged individuals (22 males and 28 females; average age 68.2 ± 3.5 years; age range = 63–76 years)[5]. These data were collected at successively, although they were published years apart. All participants had normal or corrected-to-normal visual acuity (better than 20/25). Older participants underwent screening for both cognitive status and ocular health. Probable dementia was ruled out using the Mini-Mental State Examination[5]. Older participants were examined by an ophthalmologist to exclude ocular pathologies, including macular disease, glaucoma, and cataract, although some age-related ocular changes (e.g., increased lenticular density) may have been present. Additional exclusion criteria included alcoholism, stroke, and depression.

The contrast sensitivity data were obtained using the *qCSF* method. The visibility of the stimulus for second-order images, except CM, was equated to first-order stimuli based on each observer's detection threshold to ensure that the measurement would reflect genuine neural processing. For first-order stimuli, the range of tested spatial frequencies was from 1 to 14.16 c/deg, while the range of frequencies was from 0.25 to 3.54 c/deg for second-order stimuli. 100 trials were tested per test block to measure contrast sensitivity, lasting for about eight minutes. Measurements were repeated 2 times. These studies indicate no difference in sensitivity values between dominant and non-dominant eyes, so we used average data across two eyes for each measurement. Details of the stimuli generation are provided in the reports of Reynaud et al.[5,27]. The original studies[5,27] from which data were obtained were in line with the Declaration of Helsinki and approved by the ethics committee of the University of Science and Technology of China and by the Ethics Review Board of the Montreal Neurological Institute at McGill University.

Factor analysis

Factor analysis was conducted on each age group separately, which included 52 young observers and 50 older individuals. It was conducted on the combined datasets across five different stimulus types, and separately for each stimulus type. R software was used to perform factor analysis, mainly with the *psych* package's *fa* function[86]. As no significant difference was observed between each eye's sensitivity in the previous studies[5,27] and the correlation patterns between dominant and non-dominant eyes were highly similar (Fig. S4), we analyzed average sensitivity data across two eyes (dominant and non-dominant eyes). To obtain loading scores, we used the principal component method of estimation in factor analysis. We confirmed that there was a robust correlation structure in each dataset and that it was appropriate for factor analysis using preliminary statistical tests (Bartlett's test of sphericity: P's < 0.001). Factor solutions were rotated using the varimax method, maximizing the variance of squared loadings and boosting the interpretability of statistical results[87]. To determine the number of factors, we used standard factor extraction methods to determine the number of latent sources of inter-subject variability in sensitivity data, including parallel analysis, Guttman criterion, and systematic loadings. To determine the robustness of our factor models, we visually assessed them by plotting the correlation matrices of raw data, models, and residuals, and determined that our models were robust if they captured important correlation structures of the raw data (see Fig. S2 as an example). The correlation structure of each factor in our factor model was computed through $L_f L_f' + U_f$, where L is the factor loadings matrix, and U indicates the degree of uniqueness from the factor model. This method is similar to those applied in the study of Emery et al.[18]. Correlation matrices were plotted using the *ggcorrplot* package[88]. To confirm whether loading scores were different between the two age groups, multi-group confirmatory factor analysis and likelihood ratio tests were conducted using the *lavaan* package[89].

Predicting fitted values from a factor model

Besides the traditional tests to determine the number of factors, we also evaluated the quality of the factor model's fits against the raw data by generating predicting values. The fitted values were calculated from weights, which were computed with the following equation:

$$\beta = X + y \tag{1}$$

where β is the weight of each factor at each level of a variable (i.e., spatial frequency), X^+ is the Moore–Penrose pseudo-inverse of each factor's loadings, and y is the matrix of the experimental data (Reynaud et al.; Friston et al.). A matrix multiplication of the coefficient weights β and the loading matrix yielded fitted values:

$$\hat{y} = X\beta \tag{2}$$

where X is the loading score, and ŷ is the fitted value of the sensitivity data based on the factor model.

Computational modeling for derivation of spatial channels

The spatial frequency tuning of each factor channel was estimated using the loadings from factor analysis with the formula below[28]:

$$S_n(f) = \frac{S_{obs}(f)}{\left|\frac{1}{L_n(f)}\right|^{1/Q}} \tag{3}$$

where $S_{obs}(f)$ denotes observed contrast sensitivity at spatial frequency f (raw data), $L_n(f)$ reflects loading score for channel n at frequency f, and Q is an exponent (fixed to 4) that controls the shape of the fitted function[90,91]. The derived sensitivity values $S_n(f)$ were fitted to Wilson's model[92] to extrapolate each factor's tuning function (i.e., spatial channel) as shown below:

$$S(f) = A \times \left[\exp\left(-\frac{f^2}{\sigma_1^2}\right) - B \times \exp\left(-\frac{f^2}{\sigma_2^2}\right) + C \times \exp\left(-\frac{f^2}{\sigma_3^2}\right)\right] \tag{4}$$

where A refers to the amplitude scaling factor, B denotes suppression weight, and C reflects secondary excitatory weight. Additionally, σ_1, σ_2, and σ_3 are bandwidth parameters that control the spread of the Gaussian functions. The six parameters were estimated via optimization using an Nelder–Mead algorithm. Data from each observer and the average were fitted up to 2000 times each with random starting values. Parameters that yielded the smallest residual sum of squares were chosen. Plots were visualized using *ggplot2*[93], and individual plot objects were combined into multi-panel figures using *cowplot*[94] and *smplot2*[95] in R software.

Data availability

The datasets are available online (https://mvr.mcgill.ca/AlexR/data_en.html).

Code availability

The software and routines to perform factor analysis are described in online documentation (Chapter 16 in https://smin95.github.io/dataviz).

Received: 25 November 2025; Accepted: 17 March 2026;
Published online: 01 April 2026

References

1. Nichols, E. et al. Estimation of the global prevalence of dementia in 2019 and forecasted prevalence in 2050: an analysis for the Global Burden of Disease Study 2019. *Lancet Public Health*. **7**, e105–e125 (2022).
2. Derefeldt, G., Lennerstrand, G. & LUNDH, B. Age variations in normal human contrast sensitivity. *Acta Ophthalmol.* **57**, 679–690 (1979).
3. Owsley, C., Sekuler, R. & Siemsen, D. Contrast sensitivity throughout adulthood. *Vis. Res.* **23**, 689–699 (1983).
4. Owsley, C. Aging and vision. *Vis. Res.* **51**, 1610–1622 (2011).
5. Reynaud, A., Tang, Y., Zhou, Y. & Hess, R. F. Second-order visual sensitivity in the aging population. *Aging Clin. Exp. Res.* **31**, 705–716 (2019).
6. Tang, Y. & Zhou, Y. Age-related decline of contrast sensitivity for second-order stimuli: earlier onset, but slower progression, than for first-order stimuli. *J. Vis.* **9**, 18–18 (2009).
7. Baker, C. L. & Mareschal, I. Processing of second-order stimuli in the visual cortex. *Prog. Brain Res.* **134**, 171–191 (2001).
8. Gharat, A. & Baker, C. L. Jr Motion-defined contour processing in the early visual cortex. *J. Neurophysiol.* **108**, 1228–1243 (2012).
9. Hallum, L. E., Landy, M. S. & Heeger, D. J. Human primary visual cortex (V1) is selective for second-order spatial frequency. *J. Neurophysiol.* **105**, 2121–2131 (2011).
10. Larsson, J., Heeger, D. J. & Landy, M. S. Orientation selectivity of motion-boundary responses in human visual cortex. *J. Neurophysiol.* **104**, 2940–2950 (2010).
11. Larsson, J., Landy, M. S. & Heeger, D. J. Orientation-selective adaptation to first-and second-order patterns in human visual cortex. *J. Neurophysiol.* **95**, 862–881 (2006).
12. Mareschal, I. & Baker, C. L. Jr. Cortical processing of second-order motion. *Vis. Neurosci.* **16**, 527–540 (1999).
13. Dobkins, K. R., Gunther, K. L. & Peterzell, D. H. What covariance mechanisms underlie green/red equiluminance, luminance contrast sensitivity and chromatic (green/red) contrast sensitivity? *Vis. Res.* **40**, 613–628 (2000).
14. Peterzell, D. H. & Teller, D. Y. Spatial frequency tuned covariance channels for red–green and luminance-modulated gratings: psychophysical data from human adults. *Vis. Res.* **40**, 417–430 (2000).
15. Emery, K. J., Volbrecht, V. J., Peterzell, D. H. & Webster, M. A. Variations in normal color vision. VI. Factors underlying individual differences in hue scaling and their implications for models of color appearance. *Vis. Res.* **141**, 51–65 (2017).
16. Mollon, J. D., Bosten, J. M., Peterzell, D. H. & Webster, M. A. Individual differences in visual science: what can be learned and what is good experimental practice? *Vis. Res.* **141**, 4–15 (2017).
17. Peterzell, D. H., Serrano-Pedraza, I., Widdall, M. & Read, J. C. Thresholds for sine-wave corrugations defined by binocular disparity in random dot stereograms: factor analysis of individual differences reveals two stereoscopic mechanisms tuned for spatial frequency. *Vis. Res.* **141**, 127–135 (2017).
18. Emery, K. J., Volbrecht, V. J., Peterzell, D. H. & Webster, M. A. Fundamentally different representations of color and motion revealed by individual differences in perceptual scaling. *Proc. Natl. Acad. Sci. USA*. **120**, e2202262120 (2023).
19. Reynaud, A. & Hess, R. F. Characterization of spatial frequency channels underlying disparity sensitivity by factor analysis of population data. *Front. Comput. Neurosci.* **11**, 63 (2017).
20. Min, S. H. & Reynaud, A. Applying resampling and visualization methods in factor analysis to model human spatial vision. *Investig. Ophthalmol. Vis. Sci.* **65**, 17–17 (2024).
21. Reynaud, A. & Min, S. H. Spatial frequency channels depend on stimulus bandwidth in normal and amblyopic vision: an exploratory factor analysis. *Front. Comput. Neurosci.* **17**, 1241455 (2023).
22. Legge, G. E. & Foley, J. M. Contrast masking in human vision. *J. Opt. Soc. Am.* **70**, 1458–1471 (1980).
23. Landy, M. S. & Oruç İ. Properties of second-order spatial frequency channels. *Vis. Res.* **42**, 2311–2329 (2002).
24. Oruç, I., Landy, M. S. & Pelli, D. G. Noise masking reveals channels for second-order letters. *Vis. Res.* **46**, 1493–1506 (2006).
25. Hou, F. et al. qCSF in clinical application: efficient characterization and classification of contrast sensitivity functions in amblyopia. *Investig. Ophthalmol. Vis. Sci.* **51**, 5365–5377 (2010).
26. Lesmes, L. A., Lu, Z.-L., Baek, J. & Albright, T. D. Bayesian adaptive estimation of the contrast sensitivity function: the quick CSF method. *J. Vis.* **10**, 17–17 (2010).
27. Reynaud, A., Tang, Y., Zhou, Y. & Hess, R. F. A normative framework for the study of second-order sensitivity in vision. *J. Vis.* **14**, 3–3 (2014).
28. Peterzell, D. H. Discovering sensory processes using individual differences: a review and factor analytic manifesto. *Electron. Imaging* **28**, 1–11 (2016).
29. Zhou, J., Georgeson, M. A. & Hess, R. F. Linear binocular combination of responses to contrast modulation: contrast-weighted summation in first-and second-order vision. *J. Vis.* **14**, 24–24 (2014).
30. Schofield, A. J. & Georgeson, M. A. Sensitivity to contrast modulation: the spatial frequency dependence of second-order vision. *Vis. Res.* **43**, 243–259 (2003).
31. Ledgeway, T. & Hutchinson, C. V. The influence of spatial and temporal noise on the detection of first-order and second-order orientation and motion direction. *Vis. Res.* **45**, 2081–2094 (2005).
32. Motoyoshi, I. & Kingdom, F. A. Differential roles of contrast polarity reveal two streams of second-order visual processing. *Vis. Res.* **47**, 2047–2054 (2007).
33. Peterzell, D. H., Chang, S. K. & Teller, D. Y. Spatial frequency tuned covariance channels for red–green and luminance-modulated gratings: psychophysical data from human infants. *Vis. Res.* **40**, 431–444 (2000).
34. Elliott, S. & Peterzell, D. Individual differences in contrast sensitivity functions with and without adaptive optics: direct estimates of optical and neural processes in young and elderly adults using factor analysis. *J. Vis.* **17**, 791–791 (2017).
35. Ledgeway, T. & Smith, A. T. Evidence for separate motion-detecting mechanisms for first-and second-order motion in human vision. *Vis. Res.* **34**, 2727–2740 (1994).
36. El-Shamayleh, Y. & Movshon, J. A. Neuronal responses to texture-defined form in macaque visual area V2. *J. Neurosci.* **31**, 8543–8555 (2011).
37. Kastner, S., De Weerd, P. & Ungerleider, L. G. Texture segregation in the human visual cortex: a functional MRI study. *J. Neurophysiol.* **83**, 2453–2457 (2000).
38. Merigan, W. H. Cortical area V4 is critical for certain texture discriminations, but this effect is not dependent on attention. *Vis. Neurosci.* **17**, 949–958 (2000).
39. Delahunt, P. B., Hardy, J. L. & Werner, J. S. The effect of senescence on orientation discrimination and mechanism tuning. *J. Vis.* **8**, 5–5 (2008).
40. Govenlock, S. W., Taylor, C. P., Sekuler, A. B. & Bennett, P. J. The effect of aging on the orientational selectivity of the human visual system. *Vis. Res.* **49**, 164–172 (2009).
41. Pilz, K. S., Äijälä, J. M. & Manassi, M. Selective age-related changes in orientation perception. *J. Vis.* **20**, 13–13 (2020).
42. Smith, A. T., Greenlee, M. W., Singh, K. D., Kraemer, F. M. & Hennig, J. The processing of first-and second-order motion in human visual cortex assessed by functional magnetic resonance imaging (fMRI). *J. Neurosci.* **18**, 3816–3830 (1998).
43. Noguchi, Y., Kaneoke, Y., Kakigi, R., Tanabe, H. C. & Sadato, N. Role of the superior temporal region in human visual motion perception. *Cereb. Cortex* **15**, 1592–1601 (2005).
44. Park, D. C. et al. Aging reduces neural specialization in ventral visual cortex. *Proc. Natl. Acad. Sci. USA* **101**, 13091–13095 (2004).

45. Park, J. et al. Neural broadening or neural attenuation? Investigating age-related dedifferentiation in the face network in a large lifespan sample. *J. Neurosci.* **32**, 2154–2158 (2012).
46. Voss, M. W. et al. Dedifferentiation in the visual cortex: an fMRI investigation of individual differences in older adults. *Brain Res.* **1244**, 121–131 (2008).
47. Koen, J. D., Srokova, S. & Rugg, M. D. Age-related neural dedifferentiation and cognition. *Curr. Opin. Behav. Sci.* **32**, 7–14 (2020).
48. St-Laurent, M., Abdi, H., Bondad, A. & Buchsbaum, B. R. Memory reactivation in healthy aging: evidence of stimulus-specific dedifferentiation. *J. Neurosci.* **34**, 4175–4186 (2014).
49. Andrews-Hanna, J. R. et al. Disruption of large-scale brain systems in advanced aging. *Neuron* **56**, 924–935 (2007).
50. Chan, M. Y., Park, D. C., Savalia, N. K., Petersen, S. E. & Wig, G. S. Decreased segregation of brain systems across the healthy adult lifespan. *Proc. Natl. Acad. Sci. USA* **111**, E4997–E5006 (2014).
51. Wig, G. S. Segregated systems of human brain networks. *Trends Cogn. Sci.* **21**, 981–996 (2017).
52. Bang, J. W. et al. GABA decrease is associated with degraded neural specificity in the visual cortex of glaucoma patients. *Commun. Biol.* **6**, 679 (2023).
53. Bosten, J. et al. An exploratory factor analysis of visual performance in a large population. *Vis. Res.* **141**, 303–316 (2017).
54. Ward, J., Rothen, N., Chang, A. & Kanai, R. The structure of inter-individual differences in visual ability: evidence from the general population and synaesthesia. *Vis. Res.* **141**, 293–302 (2017).
55. Shaqiri, A. et al. No evidence for a common factor underlying visual abilities in healthy older people. *Dev. Psychol.* **55**, 1775 (2019).
56. Hua, T., Kao, C., Sun, Q., Li, X. & Zhou, Y. Decreased proportion of GABA neurons accompanies age-related degradation of neuronal function in cat striate cortex. *Brain Res. Bull.* **75**, 119–125 (2008).
57. Leventhal, A. G., Wang, Y., Pu, M., Zhou, Y. & Ma, Y. GABA and its agonists improved visual cortical function in senescent monkeys. *Science* **300**, 812–815 (2003).
58. Schmolesky, M. T., Wang, Y., Pu, M. & Leventhal, A. G. Degradation of stimulus selectivity of visual cortical cells in senescent rhesus monkeys. *Nat. Neurosci.* **3**, 384–390 (2000).
59. Betts, L. R., Taylor, C. P., Sekuler, A. B. & Bennett, P. J. Aging reduces center-surround antagonism in visual motion processing. *Neuron* **45**, 361–366 (2005).
60. Yoon, J. H. et al. GABA concentration is reduced in visual cortex in schizophrenia and correlates with orientation-specific surround suppression. *J. Neurosci.* **30**, 3777–3781 (2010).
61. Hallum, L. E. & Movshon, J. A. Surround suppression supports second-order feature encoding by macaque V1 and V2 neurons. *Vis. Res.* **104**, 24–35 (2014).
62. Pitchaimuthu, K. et al. Occipital GABA levels in older adults and their relationship to visual perceptual suppression. *Sci. Rep.* **7**, 14231 (2017).
63. Abuleil, D., McCulloch, D. & Thompson, B. Visual cortex cTBS increases mixed percept duration while a-tDCS has no effect on binocular rivalry. *PLoS ONE* **16**, e0239349 (2021).
64. Steel, A., Mikkelsen, M., Edden, R. A. & Robertson, C. E. Regional balance between glutamate+ glutamine and GABA+ in the resting human brain. *Neuroimage* **220**, 117112 (2020).
65. Min, S. H. et al. Metaplasticity: dark exposure boosts local excitability and visual plasticity in adult human cortex. *J. Physiol.* **601**, 4105–4120 (2023).
66. Silvestre, D., Arleo, A. & Allard, R. Internal noise sources limiting contrast sensitivity. *Sci. Rep.* **8**, 2596 (2018).
67. Allard, R., Renaud, J., Molinatti, S. & Faubert, J. Contrast sensitivity, healthy aging and noise. *Vis. Res.* **92**, 47–52 (2013).
68. Pelli, D. G. Uncertainty explains many aspects of visual contrast detection and discrimination. *J. Opt. Soc. Am. A* **2**, 1508–1532 (1985).
69. Pestilli, F., Viera, G. & Carrasco, M. How do attention and adaptation affect contrast sensitivity? *J. Vis.* **7**, 9–9 (2007).
70. Yan, F.-F. et al. Aging affects gain and internal noise in the visual system. *Sci. Rep.* **10**, 6768 (2020).
71. Commodari, E. & Guarnera, M. Attention and aging. *Aging Clin. Exp. Res.* **20**, 578–584 (2008).
72. Dully, J., McGovern, D. P. & O'Connell, R. G. The impact of natural aging on computational and neural indices of perceptual decision making: a review. *Behav. Brain Res.* **355**, 48–55 (2018).
73. Ellemberg, D., Allen, H. A. & Hess, R. F. Second-order spatial frequency and orientation channels in human vision. *Vis. Res.* **46**, 2798–2803 (2006).
74. Fabrigar, L. R., Wegener, D. T., MacCallum, R. C. & Strahan, E. J. Evaluating the use of exploratory factor analysis in psychological research. *Psychol. Methods* **4**, 272 (1999).
75. Franco-Martínez, A., Alvarado, J. M. & Sorrel, M. A. Range restriction affects factor analysis: Normality, estimation, fit, loadings, and reliability. *Educ. Psychol. Meas.* **83**, 262–293 (2023).
76. Hutchinson, C. V. & Ledgeway, T. Sensitivity to spatial and temporal modulations of first-order and second-order motion. *Vis. Res.* **46**, 324–335 (2006).
77. Khaytin, I. et al. Functional organization of temporal frequency selectivity in primate visual cortex. *Cereb. Cortex* **18**, 1828–1842 (2008).
78. Bennett, P. J., Sekuler, R. & Sekuler, A. B. The effects of aging on motion detection and direction identification. *Vis. Res.* **47**, 799–809 (2007).
79. Billino, J., Bremmer, F. & Gegenfurtner, K. R. Differential aging of motion processing mechanisms: evidence against general perceptual decline. *Vis. Res.* **48**, 1254–1261 (2008).
80. Kelly, D. H. Motion and vision. II. Stabilized spatio-temporal threshold surface. *J. Opt. Soc. Am.* **69**, 1340–1349 (1979).
81. Solberg, J. L. & Brown, J. M. No sex differences in contrast sensitivity and reaction time to spatial frequency. *Percept. Mot. Skills* **94**, 1053–1055 (2002).
82. Shaqiri, A. et al. Sex-related differences in vision are heterogeneous. *Sci. Rep.* **8**, 7521 (2018).
83. Murray, S. O. et al. Sex differences in visual motion processing. *Curr. Biol.* **28**, 2794–2799 (2018).
84. Liu, D.-Y. et al. Sex differences in the human brain related to visual motion perception. *Biol. Sex. Differ.* **15**, 92 (2024).
85. Mateus, C. et al. Aging of low and high level vision: from chromatic and achromatic contrast sensitivity to local and 3D object motion perception. *PLoS ONE* **8**, e55348 (2013).
86. Revelle, W. Package 'psych'. *Compr. R. Arch. Netw.* **337**, 161–165 (2015).
87. Gorsuch, R. L. *Factor Analysis: Classic Edition*. (Routledge, 2014).
88. Kassambara, A. Package 'ggcorrplot'. *R. Package Version* **0**, 908 (2019).
89. Rosseel, Y. lavaan: an R package for structural equation modeling. *J. Stat. Softw.* **48**, 1–36 (2012).
90. Peterzell, D. H., Werner, J. S. & Kaplan, P. S. Individual differences in contrast sensitivity functions: the first four months of life in humans. *Vis. Res.* **33**, 381–396 (1993).
91. Sekuler, R., Wilson, H. R. & Owsley, C. Structural modeling of spatial vision. *Vis. Res.* **24**, 689–700 (1984).
92. Wilson, H. R. & Gelb, D. J. Modified line-element theory for spatial-frequency and width discrimination. *J. Opt. Soc. Am. A* **1**, 124–131 (1984).
93. Wickham, H. et al. Welcome to the tidyverse. *J. Open Source Softw.* **4**, 1686 (2019).
94. Wilke, C. O. *Fundamentals of Data Visualization: A Primer on Making Informative and Compelling Figures*. (O'Reilly Media, 2019).
95. Min, S. H. Visualization of composite plots in R using a programmatic approach and smplot2. *Adv. Methods Pract. Psychol. Sci.* **7**, 25152459241267927 (2024).

Acknowledgements
This work was support by a grant from the National Natural Science Foundation of China (32350410414) and a start-up fund (25062241-Y) from Zhejiang Sci-Tech University to S.M., and a start-up fund from the Research Institute of the McGill University Health Center to A.R.

Author contributions
A.R. conceptualized the project, S.M. performed data analyses and visualizations, and wrote the original version of the paper. Both S.M. and A.R. revised and approved the manuscript.

Competing interests
The authors declare no competing interests.

Additional information
Supplementary information The online version contains supplementary material available at https://doi.org/10.1038/s41514-026-00374-w.

Correspondence and requests for materials should be addressed to Seung Hyun Min.